Safe Sequential Path Planning of Multi-Vehicle Systems Under Presence of Disturbances and Imperfect Information

Somil Bansal*, Mo Chen*, Jaime F. Fisac, and Claire J. Tomlin

***Abstract*— Multi-UAV systems are safety-critical, and guarantees must be made to ensure no undesirable configurations such as collisions occur. Hamilton-Jacobi (HJ) reachability is ideal for analyzing such safety-critical systems because it provides safety guarantees and is flexible in terms of system dynamics; however, its direct application is limited to small-scale systems of no more than two vehicles because of the exponentially-scaling computation complexity. By assigning vehicle priorities, the sequential path planning (SPP) method allows multi-vehicle path planning to be done with a computation complexity that scales linearly with the number of vehicles. Previously the SPP method assumed no disturbances in the vehicle dynamics, and that every vehicle has perfect knowledge of the position of higher-priority vehicles. In this paper, we make SPP more practical by providing three different methods for accounting for disturbances in dynamics and imperfect knowledge of higher-priority vehicles' states. Each method has advantages and disadvantages with different assumptions about information sharing. We demonstrate our proposed methods in simulations.**

I. Introduction

Recently, there has been an immense surge of interest in using unmanned aerial vehicles (UAVs) for civil purposes. The applications of UAVs extend well beyond package delivery, and include aerial surveillance, disaster response, and other important tasks [1]–[5]. Many of these applications will involve UAVs flying in an urban environment, potentially in close proximity of humans. As a result, government agencies such as the Federal Aviation Administration (FAA) and National Aeronautics and Space Administration (NASA) of the United States are urgently trying to develop new scalable ways to organize an air space in which potentially thousands of UAVs can fly [6]–[8].

One essential problem that needs to be addressed is how a group of vehicles in the same vicinity can reach their destinations while avoiding collision with each other. Several previous studies have attempted to address this problem. In some of these studies, specific control strategies for the vehicles or moving entities are assumed, and approaches such as induced velocity obstacles have been used [9]–[11]. Other researchers have used ideas involving virtual potential fields to maintain collision avoidance while maintaining a specific formation [12], [13]. Although interesting results emerge from these previous studies, simultaneous trajectory planning and collision avoidance are not considered.

In the past, trajectory planning and collision avoidance problems in safety-critical systems have been studied using reachability analysis, which provides guarantees on the success and safety of optimal system trajectories [14]–[19]. In reachability analysis, one computes the reachable set, defined as the set of states from which the system can be driven to a target set. Reachability analysis has been successfully used in applications involving systems with no more than two vehicles, such as pairwise collision avoidance [15], automated in-flight refueling [20], two-player reach-avoid games [21], and many others [22].

Despite the advantages of reachability analysis, it cannot be directly applied to scenarios involving complex high dimensional systems such as multi-vehicle systems. The computation of reachable sets involves solving a Hamilton-Jacobi (HJ) partial differential equation (PDE) on a grid representing a discretization of the state space, causing an exponential scaling of computation complexity with respect to the dimension of the system, or roughly speaking, with the number of vehicles present. In [23], the authors presented the sequential path planning (SPP), in which vehicles are assigned a strict priority ordering. Higher-priority vehicles ignore the lower-priority vehicles, who must take into account the presence of higher-priority vehicles by treating them as induced time-varying obstacles. Under this structure, computation complexity scales just *linearly* with the number of vehicles. In addition, such a structure has the potential to flexibly divide up the airspace for the use of many UAVs, which is an important task in NASA's concept of operations for unmanned aerial systems traffic management [8]. However, the previous formulation assumes an absense of disturbances and perfect information about all vehicles. Unfortunately, perfect information about other vehicles' states and control strategies cannot be realistically assumed, and disturbances would make it impossible to commit to exact trajectories as required in [23].

In order for any path planning scheme to be viable, perfect information cannot be assumed, and disturbances must be accounted for. To take advantage of the computation benefits of the SPP scheme while resolving some of its practical challenge, in this paper we accomplish the following:

- Incorporate disturbances into the vehicle models,
- analyze three different assumptions on the information to which each vehicle may have access.

For each assumed information pattern, we propose a reachability-based method to compute the induced obstacles

This work has been supported in part by NSF under CPS:ActionWebs (CNS-931843), by ONR under the HUNT (N0014-08-0696) and SMARTS (N00014-09-1-1051) MURIs and by grant N00014-12-1-0609, by AFOSR under the CHASE MURI (FA9550-10-1-0567). The research of M. Chen and J. F. Fisac have received funding from the "NSERC" program and "la Caixa" Foundation, respectively.

* Both authors contributed equally to this work. All authors are with the Department of Electrical Engineering and Computer Sciences, University of California, Berkeley. {somil, mochen72, jfisac, tomlin}@eecs.berkeley.edu

that would guarantee collision avoidance as well as successful transit to the destination. We demonstrate and compare our proposed methods through numerical simulations.

II. Problem Formulation

Consider N vehicles, Q_i $i \in \{1, \ldots, n\}$, whose joint dynamics described by the ordinary differential equation

$$\begin{aligned} \dot{x}_i &= f_i(t, x_i, u_i, d_i), \quad t \in [t_i^{\text{EDT}}, t_i^{\text{STA}}] \\ u_i &\in \mathcal{U}_i, d_i \in \mathcal{D}_i, \quad i = 1, \ldots, N \end{aligned} \tag{1}$$

where $x_i \in \mathbb{R}^{n_i}$ is the state of the ith vehicle, u_i is the control of the ith vehicle, and d_i is the disturbance experienced by the ith vehicle. In general, the physical meaning of x_i and the dynamics f_i depend on the specific dynamic model of vehicle i, and need not be the same across the different vehicles.

We assume that the control functions $u_i(\cdot), d_i(\cdot)$ are drawn from the set of measurable functions[1]. In addition, we assume that the disturbances $d_i(\cdot)$ are drawn from Γ, the set of non-anticipative strategies [15], defined as follows:

$$\begin{aligned} &\Gamma := \{\mathcal{N} : \mathbb{U}_1 \to \mathbb{U}_2 \mid u_1(r) = \hat{u}_1(r) \text{ a. e. } r \in [t, s] \\ &\Rightarrow \mathcal{N}[u_1](r) = \mathcal{N}[\hat{u}_1](r) \text{ a. e. } r \in [t, s]\} \end{aligned} \tag{2}$$

For convenience, we will use the sets $\mathbb{U}_i, \mathbb{D}_i$ to denote the set of functions from which the control and disturbance functions $u_i(\cdot), d_i(\cdot)$ can be drawn.

We assume that $f_i(t, x_i, u_i, d_i)$ is bounded, Lipschitz continuous in x_i for any fixed t, u_i, d_i, and measurable in t, u_i, d_i for each x_i. Given any initial state x_i^0 and any control function $u_i(\cdot)$, there exists a unique continuous trajectory $x_i(\cdot)$ solving (1) [24].

Let t_i^{EDT} and t_i^{STA} denote the earliest departure time and scheduled time of arrival, respectively, of vehicle i. Let $p_i \in \mathbb{R}^p$ denote the position of vehicle i; note that p_i in most practical cases would be a subset of the state x_i. Denote the rest of the states h_i, so that $x_i = (p_i, h_i)$.

Under the worst case disturbance, each vehicle aims to get to some set of target states, denoted $\mathcal{T}_i \subset \mathbb{R}^{n_i}$, at some scheduled time of arrival t_i^{STA}. On its way to $\mathcal{T}_i$, each vehicle must avoid the danger zones $\mathcal{A}_{ij}(t)$ of all other vehicles $j \neq i$ for all time. In general, the danger zone can be defined to capture any undesirable configuration between vehicle i and vehicle j. In this paper, we define $\mathcal{A}_{ij}(t)$ as

$$\mathcal{A}_{ij}(t) = \{x_i \in \mathbb{R}^{n_i} : \|p_i - p_j(t)\|_2 \leq R_c\}, \tag{3}$$

the interpretation of which is that a vehicle is another vehicle's danger zone if the two vehicles are within a Euclidean distance of R_c apart. The joint path planning problem is depicted in Fig. 1.

The problem of driving each of the vehicles in (1) into their respective target sets $\mathcal{T}_i$ would be in general a differential game of dimension $\sum_i n_i$. Due to the exponential scaling of the complexity with the problem dimension, an optimal solution is computationally intractable even for $N > 2$ with n_i as small as 3.

[1]A function $f : X \to Y$ between two measurable spaces (X, Σ_X) and (Y, Σ_Y) is said to be measurable if the preimage of a measurable set in Y is a measurable set in X, that is: $\forall V \in \Sigma_Y, f^{-1}(V) \in \Sigma_X$, with Σ_X, Σ_Y σ-algebras on X,Y.

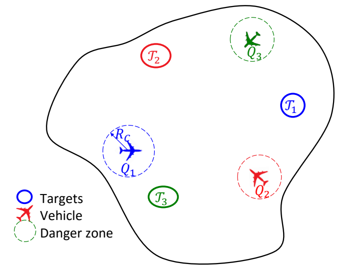

Fig. 1: Problem setup.

In this paper, we assume assigned priorities of the vehicles as in the SPP method [23]. While traveling to its target set, a vehicle may ignore the presence of lower priority vehicles, but must take full responsibility for avoiding higher priority vehicles. Since the analysis in [23] did not take into account the presence of disturbances d_i and limited information available to each vehicle, we extend the work in [23] to consider these practically important aspects of the problem. In particular, we answer the following interdependent questions that were not previously addressed:

1) How can each vehicle guarantee that it will reach its target set without getting into any danger zones, despite the disturbances it experiences?
2) How can each vehicle take into account the disturbances that other vehicles experience?
3) How should each vehicle robustly handle situations with limited information about the state and intention of other vehicles?

III. Background

This section provides a brief summary of [23], in which SPP scheme is proposed under perfect information and absence of disturbance. Here, the dynamics of Q_i becomes

$$\begin{aligned} \dot{x}_i &= f_i(t, x_i, u_i), \quad t \in [t_i^{\text{EDT}}, t_i^{\text{STA}}] \\ u_i &\in \mathcal{U}_i, \quad i = 1, \ldots, N \end{aligned} \tag{4}$$

where the difference compared to (1) is that the disturbance d_i is no longer part of the dynamics.

In order to make the N-vehicle path planning problem safe and tractable, a reasonable structure is imposed to the problem: each vehicle is assigned a strict priority ordering. When planning its trajectory to its target, a higher-priority vehicle can disregard the presence of a lower priority vehicle. In contrast, a lower priority vehicle must take into account the presence of all higher priority vehicles, and plan its trajectory in a way that avoids the higher priority vehicles' danger zones. For convenience and without lost of generality, let vehicle i have the ith highest priority and denote it as Q_i.

Under the above convention, each vehicle Q_i must take into account time-varying obstacles induced by vehicles $Q_j, j < i$, denoted $\mathcal{O}_i^j(t)$. Optimal safe path planning of each lower-priority vehicle Q_i then consists of determining the optimal path that allows Q_i to each its target $\mathcal{T}_i$ while avoiding the time-varying obstacles $\mathcal{G}_i$, defined by

$$\mathcal{G}_i(t) = \bigcup_{j=1}^{i-1} \mathcal{O}_i^j(t) \tag{5}$$

Such an optimal path planning problem can be solved by computing a backward reachable set (BRS) $\mathcal{V}_i(t)$ from a target set $\mathcal{T}_i$ using formulations of HJ variational inequalities (VI) such as [14], [16], [17], [19]. To compute BRSs under the presence of time-varying obstacles, the authors in [17] augmented system with the time variable, and then applied reachability theory for time-invariant systems. To avoid increasing the problem dimension and save computation time, for the simulations of this paper we utilized the formulation in [19], which does not require augmentation of the state space with the time variable.

Starting from the highest-priority vehicle Q_1, one computes the BRS $\mathcal{V}_1(t)$, from which the optimal control and optimal trajectory $x_1(\cdot)$ to the target $\mathcal{T}_1$ can be obtained. Under the absence of disturbances and perfect information, the obstacles induced by Q_1 for lower-priority vehicle Q_i is simply the danger zone centered around the position of each point $p_1(\cdot)$ on the trajectory:

$$\mathcal{O}_i^1(t) = \{x_j : \|p_j - p_1(\cdot)\| \leq R_c\} \tag{6}$$

Given $\mathcal{O}_i^j(t), j < i$, and continuing with $i = 2$, the optimal safe trajectories for each vehicle Q_i can be computed. All of the trajectories are optimal in the sense that given the requirement that Q_i must arrive at $\mathcal{T}_i$ at time t_i^{STA}, the latest departure time t_i^{LDT} and the optimal control $u_i^*(\cdot)$ that guarantees arrival at t_i^{STA} can be obtained.

To compute $\mathcal{V}_i(t)$ using the method in [19], we solve the following HJ VI:

$$\begin{aligned} \max\Big\{ &\min\left\{D_t V_i(t,x_i) + H_i\left(t,x_i,D_{x_i}V_i\right),\right.\\ &\left. l_i(x_i) - V_i(t,x_i)\right\}, -g_i(t,x_i) - V_i(t,x_i)\Big\} = 0 \\ &t \in [t^{\text{EDT}}, t^{\text{STA}}] \\ &V_i(t^{\text{STA}}, x_i) = \max\left\{l_i(x_i), -g_i(0,x_i)\right\}, \text{with} \end{aligned} \tag{7}$$

$$H_i\left(t,x_i,p\right) = \min_{u_i \in \mathcal{U}} p \cdot f_i(t,x_i,u_i) \tag{8}$$

where $l_i(x_i), g_i(t,x_i), V_i(t,x_i)$ are implicit surface functions representing the target $\mathcal{T}_i$, the time-varying obstacles $\mathcal{G}_i(t)$, and the backward reachable set $\mathcal{V}_i(t)$, respectively:

$$\begin{aligned} x_i \in \mathcal{T}_i &\Leftrightarrow l_i(x_i) \leq 0 \\ x_i(t) \in \mathcal{G}_i(t) &\Leftrightarrow g_i(t,x_i) \leq 0 \\ x_i(t) \in \mathcal{V}_i(t) &\Leftrightarrow V_i(t,x_i) \leq 0 \end{aligned} \tag{9}$$

The optimal control is given by

$$u_i^*\left(t,x_i\right) = \arg\min_{u_i \in \mathcal{U}} D_{x_i}V_i(t,x_i) \cdot f_i(t,x_i,u_i) \tag{10}$$

IV. Disturbances and Incomplete Information

Disturbances and incomplete information significantly complicates the SPP scheme. The main differences are as follows:

1) The vehicle dynamics satisfy (1) as opposed to (4).
2) Committing to exact trajectories is no longer possible, since the disturbance $d_i(\cdot)$ is a priori unknown.
3) The induced obstacles $\mathcal{O}_i^j(t)$ are no longer just the danger zones centered around positions.

We present three methods for address the above issues. Each method has its advantages and disadvantages depending on the situation. The three methods are as follows:

- Centralized control: A specific control strategy is enforced upon a vehicle; this can be achieved, for example, by some central agent such as an air traffic controller.
- Least restrictive control: A lower-priority vehicle assumes that higher-priority vehicles will arrive at their targets on time, but has no other information.
- Robust trajectory tracking: Each vehicle declares a nominal trajectory which can be robustly tracked under disturbances.

In general, the above methods can be used in combination in a single path planning problem, with each vehicle independently having different assumptions about each higher-priority vehicle. For clarity, we will present each method as if all vehicles are using the same method of path planning.

In addition, for simplicity and clarity of explanation, we will assume that no static obstacles exist. In the situations where static obstacles do exist, the time-varying obstacles $\mathcal{G}_i(t)$ simply becomes the union of the induced obstacles $\mathcal{O}_i^j(t)$ in (5) and the static obstacles.

A. Method 1: Centralized Controller

The highest-priority vehicle Q_1 first plans its path by computing the BRS (with $i = 1$)

$$\begin{aligned} \mathcal{V}_i(t) = \{x_i :\, &\exists u_i(\cdot) \in \mathbb{U}, \forall d_i(\cdot) \in \mathbb{D}, x_i(\cdot) \text{ satisfies (1)}, \\ &\forall s \in [t_i^{\text{EDT}}, t_i^{\text{STA}}], x_i(s) \notin \mathcal{G}_i(s), \\ &\exists s \in [t_i^{\text{EDT}}, t_i^{\text{STA}}], x_i(s) \in \mathcal{T}_i\} \end{aligned} \tag{11}$$

Since we have assumed no static obstacles exist, we have that for $Q_1, \mathcal{G}_1(s) = \emptyset \; \forall s \in [t_i^{\text{EDT}}, t_i^{\text{STA}}]$, and thus the above BRS is well-defined. This BRS can be computed by solving the HJ VI (7) with the following Hamiltonian:

$$H_i\left(t,x_i,p\right) = \min_{u_i \in \mathcal{U}} \max_{d_i \in \mathcal{D}} p \cdot f_i(t,x_i,u_i,d_i) \tag{12}$$

where $l_i(x_i), g_i(t,x_i), V_i(t,x_i)$ are implicit surface functions representing the target $\mathcal{T}_i, \mathcal{G}_i(t), \mathcal{V}_i(t)$, respectively. From the BRS, we can obtain the optimal control

$$u_i^*(t,x_i) = \arg\min_{u_i \in \mathcal{U}} \max_{d_i \in \mathcal{D}} p \cdot f_i(t,x_i,u_i,d_i^*) \tag{13}$$

The latest departure time t^{LDT} is then given by $\arg\inf_t x_i(t^{\text{EDT}}) \in \mathcal{V}_i(t)$.

If there is a centralized controller directly controlling each of the N vehicles, then the control law of each vehicle can be enforced. In this case, lower priority vehicles can safely assume that higher priority vehicles are applying the enforced control law. In particular, the optimal controller for getting to the target, $u_i^*(t,x)$ can be enforced. In this case, the dynamics of each vehicle becomes

$$\dot{x}_i = f_i^*(t, x_i, d_i) = f_i(t, x_i, u_i^*(t, x), d_i)$$
$$d_i \in \mathcal{D}_i \quad i = 1, \dots, N, \quad t \in [t_i^{\text{LDT}}, t_i^{\text{STA}}] \tag{14}$$

where u_i no longer appears explicitly in the dynamics.

From the perspective of a lower-priority vehicle Q_i, a higher-priority vehicle $Q_j, j < i$ induces an time-varying obstacle that represents the positions that could possibly be within the capture radius R_c of Q_j under the dynamics $f_j^*(t, x_j, d_j)$. Determining this obstacle involves computing a forward reachable set (FRS) of Q_j starting from $x_j(t^{\text{LDT}})$. The FRS $\mathcal{W}_j(t)$ is defined as follows:

$$\begin{aligned} \mathcal{W}_j(t) = \{&y \in \mathbb{R}^{n_j} : \exists d_j(\cdot) \in \mathbb{D}_j, \\ &x_j(\cdot) \text{ satisfies (14)}, \, x_j(t) = y\} \end{aligned} \tag{15}$$

Conveniently, the FRS can be computed using the following HJ VI:

$$\begin{aligned} &D_t W_j(t, x_j) + H_j\left(t, x_j, D_{x_j} W\right) = 0, t \in [t_j^{\text{LDT}}, t_j^{\text{STA}}] \\ &W_j(t_j^{\text{LDT}}, x_j) = \bar{l}_j(x_j) \end{aligned} \tag{16}$$

with the following Hamiltonian

$$H_j\left(t, x_j, p\right) = \min_{d_j \in \mathcal{D}_j} p \cdot \bar{f}_j(t, x_j, d_j) \tag{17}$$

where $\bar{l}$ is chosen to be such that[2] $\bar{l}(y) = 0 \Leftrightarrow y = x_j(t^{\text{LDT}})$.

The FRS $\mathcal{W}_j(t)$ represents the set of possible states at time t of a higher-priority vehicle Q_j given the worst case disturbance $d_j(\cdot)$ and given that Q_j uses the feedback controller $u_j^*(t, x)$. In order for a lower-priority vehicle Q_i to guarantee that it does not go within a distance of R_c to Q_j, Q_i must stay a distance of at least R_c away from the set $\mathcal{W}_j(t)$ for all possible values of the non-position states h_j. This gives the obstacle induced by a higher priority vehicle Q_j for a lower priority vehicle Q_i as follows:

$$\mathcal{O}_i^j(t) = \{x_i : \text{dist}(p_i, \mathcal{P}_j(t)) \le R_c\} \tag{18}$$

where the dist$(\cdot, \cdot)$ function represents the minimum distance from a point to a set, and the set $\mathcal{P}_j(t)$ is the set of states in the FRS $\mathcal{W}_j(t)$ projected onto the states representing position p_j, and disregarding the non-position dimensions h_j:

$$\mathcal{P}_j(t) = \{p : \exists h_j, (p, h_j) \in \mathcal{W}_j(t)\}. \tag{19}$$

Finally, taking the union of the induced obstacles $\mathcal{O}_i^j(t)$ as in (5) gives us the time-varying obstacles $\mathcal{G}_i(t)$ needed to define and determine the BRS $\mathcal{V}_i(t)$ in (11). Repeating this process, all vehicles will be able to plan paths that guarantee the vehicles' timely and safe arrival.

B. Method 2: Least Restrictive Control

Here, we again begin with the highest vehicle Q_1 planning its path by computing the BRS $\mathcal{V}_i(t)$ in (11). However, if there is no centralized controller to enforce the control policy for higher priority vehicles, weaker assumptions must be made by the lower priority vehicles to ensure collision avoidance. One reasonable assumption that a lower priority vehicle can make is that all higher priority vehicles follow the least restrictive control that would take them to their targets. This control would be given by

$$u_j(t, x_j) \in \begin{cases} \{u_j^*(t, x_j) \text{ given by (13)}\} \text{ if } x_j(t) \in \partial\mathcal{V}_j(t), \\ \mathcal{U}_i \text{ otherwise} \end{cases} \tag{20}$$

Such a controller allows each higher priority vehicle to use any controller it desires, except when it is on the boundary of the BRS, $\partial\mathcal{V}_j(t)$, in which case the optimal control $u_j^*(t, x_j)$ given by (13) must be used to get to the target on time. This assumption is the weakest assumption that could be made by lower priority vehicles given that the higher priority vehicles will get to their targets on time.

Suppose a lower priority vehicle Q_i assumes that higher priority vehicles $Q_j, j < i$ use the least restrictive control strategy (20). From the perspective of the lower priority vehicle Q_i, a higher priority vehicle Q_j could be in any state that is reachable from Q_j's initial state $x_j(t^{\text{LDT}})$ and from which the target $\mathcal{T}_j$ can be reached. Mathematically, this is defined by Q_j is the intersection of a FRS from the initial state $x_j(t^{\text{EDT}})$ and the BRS defined in (11) from the target set $\mathcal{T}_j$, $\mathcal{V}_j(t) \cap \mathcal{W}_j(t)$. In this situation, since Q_j cannot be assumed to be using any particular feedback control, $\mathcal{W}_j(t)$ is defined in (21).

$$\begin{aligned} \mathcal{W}_j(t) = \{&y \in \mathbb{R}^{n_j} : \exists u_j(\cdot) \in \mathbb{U}_j, \exists d_j(\cdot) \in \mathbb{D}_j, \\ &x_j(\cdot) \text{ satisfies (1)}, \, x_j(t) = y\} \end{aligned} \tag{21}$$

This FRS can be computed by solving (16) with

$$H_j\left(t, x_j, p\right) = \min_{u_j \in \mathcal{U}_j} \min_{d_j \in \mathcal{D}_j} p \cdot f_j(t, x_j, u_j, d_j) \tag{22}$$

In turn, the obstacle induced by a higher priority Q_j for a lower priority vehicle Q_i is as follows:

$$\begin{aligned} &\mathcal{O}_i^j(t) = \{x_i : \text{dist}(p_i, \mathcal{P}_j(t)) \le R_c\}, \text{ with} \\ &\mathcal{P}_j(t) = \{p : \exists h_j, (p, h_j) \in \mathcal{V}_j(t) \cap \mathcal{W}_j(t)\} \end{aligned} \tag{23}$$

Note that the centralized controller method described in the previous section can be thought of as the "most restrictive control" method, in which all vehicles must use the optimal controller at all times, while the least restrictive control method allows vehicles to use any suboptimal controller to get to the target on time. These two methods can be considered two extremes of a spectrum in which varying degrees of optimality is assumed for higher-priority vehicles.

C. Method 3: Robust Tracking of Nominal Trajectories

A third way of computing induced obstacles is to have vehicles commit to robustly tracking a feasible nominal trajectory. If a vehicle can be guaranteed to track a trajectory with a bounded error at all times, then this bound can be used to determine the induced obstacles. This computation can be done in two phases: the planning phase and the disturbance rejection phase. In the planning phase, a nominal trajectory is computed that is feasible in the absence of disturbances. In the disturbance rejection phase, we then compute a bound on the tracking error, caused by a vehicle's inability to exactly track the nominal trajectory in the presence of disturbances.

It is important to note that the planning phase does not make full use of the vehicle's control authority, as

[2] In practice, we define the target set to be a small region around the vehicle's initial state.

some margin is needed to reject unexpected disturbances. Therefore, in this method, planning is done for a reduced control set $\mathcal{U}^p \subset \mathcal{U}$. The resulting trajectory reference will not utilize the vehicle's full maneuverability; replicating the nominal control is therefore always possible, with additional maneuverability available at execution time to counteract external disturbances.

In this paper, we use reachability to determine the tracking error bound and can be determined independently of the nominal trajectory. To compute this error bound, we wish to find a robust control-invariant set in the joint state space of the vehicle and a tracking reference that may "maneuver" arbitrarily over time, and in the presence of an unknown bounded disturbance. Taking a worst-case approach, the tracking reference can be viewed as a virtual evader vehicle that is optimally avoiding the actual vehicle to enlarge the tracking error. We therefore can model trajectory tracking as a pursuit-evasion game in which the actual vehicle is playing against the coordinated worst-case action of the virtual vehicle and the disturbance. In general, this game will be governed by dynamics of the form:

$$\begin{aligned} &\dot{x} = f(t, x, u, d), \quad \dot{x_r} = f(t, x_r, u_r, 0), \\ &u \in \mathcal{U}, u_r \in \mathcal{U}^p, d \in \mathcal{D}, \quad t \in [0, T] \end{aligned} \tag{24}$$

where x and x_r represent the state of the actual vehicle and the virtual evader, respectively. Given an error bound $\mathcal{E}(x_{r,i})$ on the tracking error $e = x - x_r$, we define the target set $\mathcal{T}$ for this reachability problem to be the set of joint configurations where this bound is violated: $\mathcal{T} = \{(x, x_{r,i}) : x \notin \mathcal{E}(x_{r,i})\}$. In this case, the BRS $\mathcal{V}(t)$ represents the set of states from which the vehicle may be driven to violate the tracking error bounds, outside of $\mathcal{E}(x_{r,i})$.

With analogous definitions as those in Section III, $\mathcal{V}(t)$ can be characterized as the negative region of the solution V to a simpler case of (7):

$$\begin{aligned} &\min \left\{D_t V(t,z) + H\left(t,z,D_z V\right), l(t,z) - V(t,z)\right\} = 0, \\ &t \in [0,T], \qquad V(T,z) = l(T,z) \\ &H\left(t,z,p\right) = \max_{u \in \mathcal{U}} \min_{u_r \in \mathcal{U}^p} \min_{d \in \mathcal{D}} p \cdot f_z(t,z,u,u_r,d) \end{aligned} \tag{25}$$

where for compactness of notation we denote $z = (x, x_r)$ and $f_z(t, z, u, u_r, d) = [f(t, x, u, d), f(t, x_r, u_r, 0)]$. The complement of $\mathcal{V}(0)$ is the maximal robust controlled-invariant set in $\mathcal{T}^c$. Letting $T \to \infty$ we obtain the infinite controlled-invariant set, which we denote by Ω. If this set is nonempty, then the tracking error e at flight time is guaranteed to remain within $\mathcal{E}$ provided that the vehicle starts inside Ω and subsequently applies the feedback control law implicitly defined in (25):

$$\kappa(x, x_r) \in \arg\max_{u \in \mathcal{U}} \min_{u_r \in \mathcal{U}^p, d \in \mathcal{D}} p \cdot f_z(t, z, u, u_r, d). \tag{26}$$

In cases where the error dynamics are independent of the absolute state as in (27), Ω can be computed in the state space of the tracking error e to produce a feedback control law that also only depends on e, and to significantly reduce the problem dimensionality. We will present one such example in Section V.

$$\begin{aligned} &\dot{e} = f_e(t, e, u, u_r, d), \\ &u \in \mathcal{U}, u_r \in \mathcal{U}^p, d \in \mathcal{D}, \quad t \in [0, T], \end{aligned} \tag{27}$$

Given $\mathcal{E}$, we can guarantee that Q_i will reach its target $\mathcal{T}_i$ if $\mathcal{E} \subset \mathcal{T}_i$; thus, in the path planning phase, we modify $\mathcal{T}_i$ to be $\{x : \mathcal{E}(x) \subseteq \mathcal{T}_i\}$, and compute a BRS, with the control authority $\mathcal{U}^p$, that contains the initial state of the vehicle. The overall control policy to reach the destination is given by 26.

Finally, since each vehicle Q_i can only be guaranteed to stay within $\mathcal{E}(x_{r,i})$, we must make sure at any given time, the error bounds of Q_i and Q_j, $\mathcal{E}(x_{r,i})$ and $\mathcal{E}(x_{r,j})$, do not intersect. This can be done by choosing the induced obstacle to be the Minkowski sum of the error bounds (the Minkowski sum of sets A and B is the set of all points that are the sum of any point in A and B).Thus,

$$\mathcal{O}_i^j(t) = \{x_i : \text{dist}(p_i, \mathcal{P}_j(t)) \leq R_c\}, \tag{28}$$

where $\mathcal{P}_j(t)$ is given by

$$\mathcal{P}_j(t) = \{p : \exists h_j, (p, h_j) \in \mathcal{E}(0) + \mathcal{E}(x_{r,j}(t))\}, \tag{29}$$

where 0 denotes the origin.

V. Numerical Simulations

We demonstrate our proposed methods using a four-vehicle example. Each vehicle has the following simple kinematics model:

$$\begin{aligned} \dot{p}_{x,i} &= v_i \cos\theta_i + d_{x,i} \\ \dot{p}_{y,i} &= v_i \sin\theta_i + d_{y,i} \\ \dot{\theta}_i &= \omega_i + d_{\theta,i}, \\ \underline{v} &\leq v_i \leq \bar{v}, |\omega_i| \leq \bar{\omega}, \\ \|(d_{x,i}, d_{y,i})\|_2 &\leq d_r, |d_{\theta,i}| \leq \bar{d_\theta} \end{aligned} \tag{30}$$

where $p_i = (p_{x,i}, p_{y,i})$ represent vehicle Q_i's position, θ_i represents Q_i's heading, and $d = (d_{x,i}, d_{y,i}, d_{\theta,i})$ represent the disturbances in the three states. The control of Q_i is $u_i = (v_i, \omega_i)$, where v_i is the speed of Q_i and ω_i is the turn rate; both controls have a lower and upper bound. For illustration purposes, we chose $\underline{v} = 0.5, \bar{v} = 1, \bar{\omega} = 1$; however, our method can easily handle the case in which these inputs differ across vehicles and cases in which each vehicle has different dynamic models. The disturbance bounds are chosen as $d_r = 0.1$ and $\bar{d_\theta} = 0.2$, which correspond to a 10% uncertainty in the dynamics.

The initial states of the vehicles are given as follows:

$$\begin{aligned} x_1^0 &= (-0.5, 0, 0), & x_2^0 &= (0.5, 0, \pi), \\ x_3^0 &= (-0.6, 0.6, 7\pi/4), & x_4^0 &= (0.6, 0.6, 5\pi/4). \end{aligned} \tag{31}$$

Each of the vehicles have a target set $\mathcal{T}_i$ that is circular in their position p_i centered at $c_i = (c_{x,i}, c_{y,i})$ with radius r:

$$\mathcal{T}_i = \{x_i \in \mathbb{R}^3 : \|p_i - c_i\| \leq r\} \tag{32}$$

For the example shown, we chose $c_1 = (0.7, 0.2), c_2 = (-0.7, 0.2), c_3 = (0.7, -0.7), c_4 = (-0.7, -0.7)$ and $r = 0.1$. The setup of the example is shown in Fig. 2.

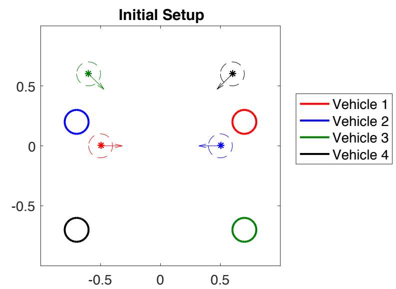

Fig. 2: Initial configuration of the four-vehicle example.

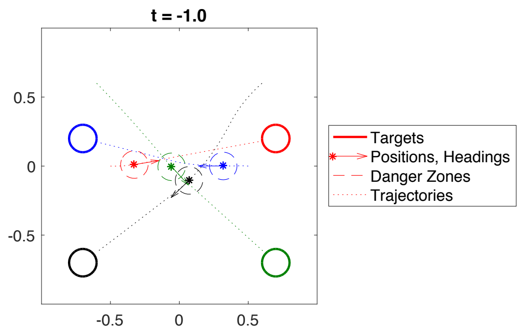

Fig. 3: Simulated trajectories in the centralized controller method. Since the higher priority vehicles induce relatively smaller obstacles in this case, vehicles do not deviate much from a straight line trajectory towards their respective targets.

Since the joint state space of this system is intractable for a direct application of HJ reachability theory, we repeatedly solve (7) to compute BRSs from the targets $\mathcal{T}_i, i = 1, 2, 3, 4$, in that order, with moving obstacles induced by vehicles $j = 1, \ldots, i-1$. We also obtain $t_i^{\text{LDT}}, i = 1, 2, 3, 4$ assuming $t_i^{\text{STA}} = 0$ without loss of generality. Note that even though t_i^{STA} is assumed to be same for all vehicles in this example for simplicity, our method can easily handle the case in which t_i^{STA} are different for each vehicle.

For each proposed method of computing induced obstacles, we show the vehicles' entire trajectories (colored dotted lines), and overlay their positions (colored asterisks) and headings (arrows) at a point in time in which they are in relatively dense configuration. In all cases, the vehicles are able to avoid each other's danger zones (colored dashed circles) while getting to their target sets in minimum time. In addition, we show the evolution of the BRS over time for Q_3 (green boundaries) as well as the induced obstacles of higher-priority vehicles (black boundaries).

A. Centralized Controller

Fig. 3 shows the simulated trajectories in the situation where a centralized controller enforces each vehicle to use the optimal controller $u_i^*(t, x_i)$ according to (13), as described in Section IV-A.

In this case, vehicles appear to deviate slightly from a straight line trajectory towards their respective targets, just enough to avoid higher priority vehicles. The deviation is small since the centralized controller is quite restrictive, making the possible positions of higher priority vehicles cover a small area. In the dense configuration at $t = -1.0$, the vehicles are close to each other but still outside each other's danger zones.

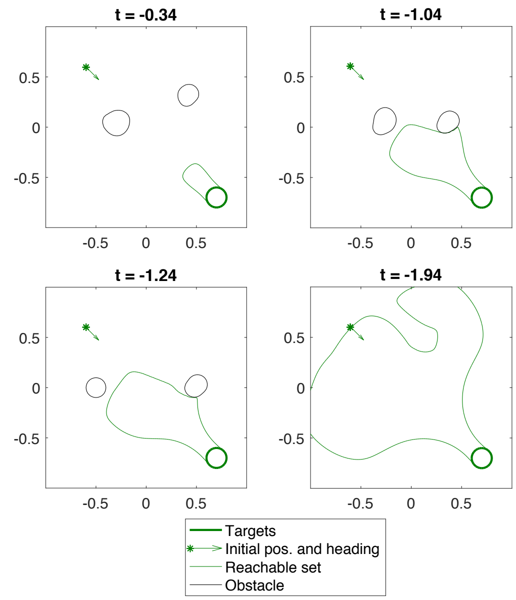

Fig. 4: Evolution of the BRS and the obstacles induced by Q_1 and Q_2 for Q_3 in the centralized controller method. Since every vehicle is applying the optimal control at all times, the obstacle sizes are relatively small.

Fig. 4 shows the evolution of the BRS for Q_3 (green boundary), as well as the obstacles (black boundary) induced by the higher priority vehicles Q_1 (blue) and Q_2 (red). The locations of the induced obstacles at different time points include the actual positions of Q_1 and Q_2 at those times, and the size of the obstacles remains relatively small. t_i^{LDT} numbers for the four vehicles (in order) in this case are $-1.35, -1.37, -1.94$ and -2.04, respectively. Numbers are relatively close for vehicles Q_1, Q_2 and Q_3, Q_4, because the obstacles generated by higher priority vehicle are small and hence do not affect t^{LDT} of the lower priority vehicles significantly.

B. Least Restrictive Control

Fig. 5 shows the simulated trajectories in the situation where each vehicle assumes that higher-priority vehicles use the least restrictive control to reach their targets, as described in IV-B. Fig. 6 shows the BRS and induced obstacles for Q_3.

Q_1 (red) takes a relatively straight path to reach its target. From the perspective of all other vehicles, large obstacles are induced by Q_1, since lower priority vehicles make the weak assumption that higher priority vehicles are using the least restrictive control. Because the obstacles induced by higher priority vehicles are so large, it is faster for lower priority vehicles to wait until higher priority vehicles pass by than to move around the higher priority vehicles. As a result, the vehicles never form a dense configuration, and their trajectories are all relatively straight, indicating that they end up taking a short path to the target after higher priority vehicles

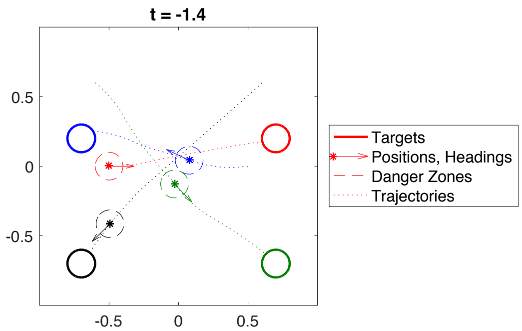

Fig. 5: Simulated trajectories in the least restrictive control method. All vehicles start moving before Q_1 starts, because the large obstacles make it optimal to wait until higher priority vehicles pass by, leading to a smaller t^{LDT}.

pass by. This is also indicated by low t_i^{LDT} numbers for the four vehicles, which are $-1.35, -1.97, -2.66$ and -3.39, respectively. Note that, compared to the centralized controller method, t_i^{LDT}s decrease significantly for all vehicles, except Q_1 for which the number does not change as it is the highest priority vehicle, and hence need not account for any moving obstacles.

From Q_3's (green) perspective, the large obstacles induced by Q_1 and Q_2 are shown in Fig. 6 as the black boundary. As the BRS (green boundary) evolves over time, its growth gets inhibited by the large obstacle for a long time, from $t = -0.89$ to $t = -1.39$. Eventually, the boundary of the BRS reaches the initial state of the green vehicle at $t = t_i^{\text{LDT}} = -2.66$.

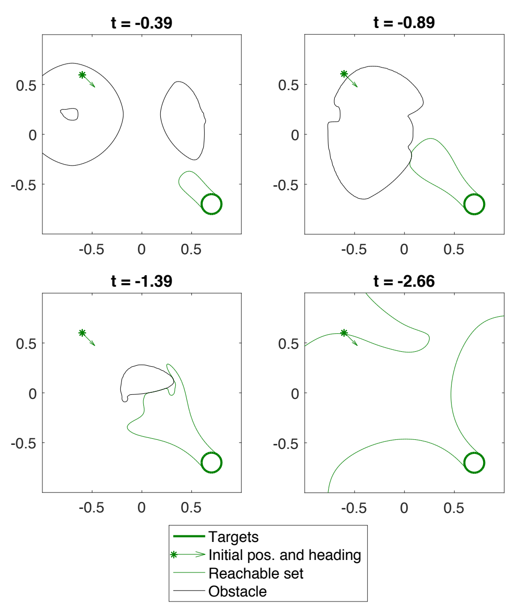

Fig. 6: Evolution of the BRS for Q_3 in the least restrictive control method. t_3^{LDT} is significantly lower than that in the centralized controller method (-1.94 vs. -2.66), reflecting the impact of bigger induced obstacles.

C. Robust Trajectory Tracking

Fig. 7 shows the vehicle trajectories in the situation where each vehicle tracks a pre-specified trajectory and is

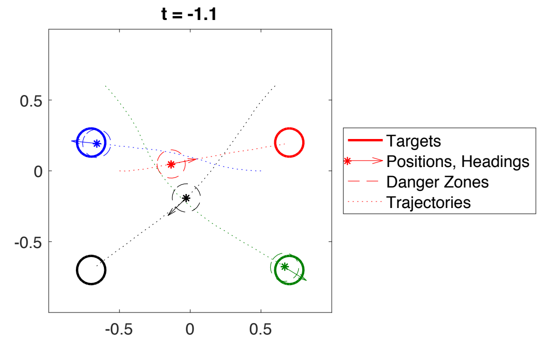

Fig. 7: Simulated trajectories for the robust trajectory tracking method.

guaranteed to stay inside a "bubble" around the trajectory. Fig. 8 shows the evolution of BRS and induced obstacles for vehicle Q_3. The obstacles induced by other vehicles inhibit the evolution of the BRS, carving out thin channels, which can be seen at $t = -2.59$, that separate the BRS into different islands. One can see how these channels and islands form by examining the time evolution of the BRS set.

t_i^{LDT} numbers for the four vehicles in this case are $-1.61, -3.16, -3.57$ and -2.47 respectively. In this method, vehicles use reduced control authority for path planning towards a reduced-size effective target set. As a result, higher-priority vehicles tend to have higher t^{LDT} compared to the other two methods, as evident from t_1^{LDT}. Because of this "sacrifice" by the higher-priority vehicles during the path planning phase, the t^{LDT} of lower priority vehicles may increase compared to that in the other methods, as evident from t_4^{LDT}. Overall, it is unclear whether t_i^{LDT} for a vehicle would increase or decrease compared to the other methods, as t_i^{LDT} is increased by a conservative path planning by higher-priority vehicles, and decreased by a conservative path planning of Q_i.

VI. Comparison of Proposed Methods

This section briefly discusses the relative advantages and limitations of the proposed obstacle generation methods. Each method makes a trade-off between optimality (in terms of t_i^{LDT}) and flexibility in control and disturbance rejection.

A. Centralized Controller

Given an order of priority, the vehicles will have the relatively high t_i^{LDT} in this method since a higher-priority vehicle maximizes its t_i^{LDT} as much as possible, while at the same time inducing a relatively small obstacle so as to minimize its impedance towards the lower-priority vehicles. A limitation of this method is that a centralized controller is likely required to ensure that the optimal control is being applied by the vehicles at all times, and hence safety.

B. Least Restrictive Control

This method gives more control flexibility to the higher priority vehicles, as long as the control does not push the vehicle out of its BRS. This flexibility, however, comes at the price of having larger induced obstacle, lowering t_i^{LDT} for the lower-priority vehicles.

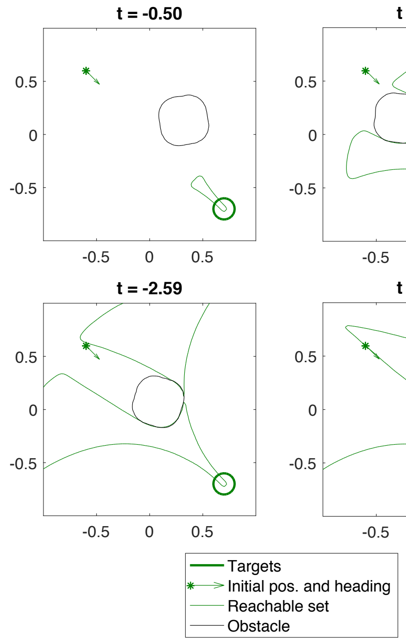

Fig. 8: Evolution of the BRS for Q_3 in the robust trajectory tracking method. As the BRS grows in time, the induced obstacles carve out a channel. Note that a smaller target set is used to compute the BRS to ensure that the vehicle reaches the target set by $t = 0$ for any allowed tracking error.

C. Robust Trajectory Tracking

Since the obstacle size is constant over time, this method is easier to implement from a practical standpoint. This method also aims at striking a balance between t_i^{LDT} across vehicles. In particular, the t_i^{LDT} of a higher priority vehicle can be lower compared to the centralized controller method, so that a lower priority vehicle can achieve a higher t^{LDT}, making this method particularly suitable for the scenarios where there is no strong sense of priority among vehicles. This method, however, is computationally tractable when the tracking error dynamics are independent of the absolute states, as it otherwise requires doing computation in the joint state space of system dynamics and virtual vehicle dynamics as defined in (24).

VII. Conclusions and Future Work

We have proposed three different methods of generating induced obstacles in the sequential path planning method; these three methods can be used independently across the different vehicles in the path planning problem. In each method, different assumptions about the control strategy of higher-priority are made. In all of the methods, all vehicles are guaranteed to successfully reach their respective destinations without entering each other's danger zones despite the worst-case disturbance the vehicles could experience. Compared to the work in [23], our proposed methods result in lower vehicle densities so that the vehicles have enough leeway to guarantee safety in the presence of disturbances and limited information. Future work includes exploring methods for fast re-planning, and making the multi-vehicle system robust to unforeseen circumstances such as the presence of intruders.

References

[1] B. P. Tice, "Unmanned aerial vehicles – the force multiplier of the 1990s," *Airpower Journal*, 1991.

[2] W. M. Debusk, "Unmanned aerial vehicle systems for disaster relief: Tornado alley," in *Infotech@Aerospace Conferences*, 2010.

[3] Amazon.com, Inc. (2016) Amazon prime air. [Online]. Available: http://www.amazon.com/b?node=8037720011

[4] AUVSI News. (2016) Uas aid in south carolina tornado investigation. [Online]. Available: http://www.auvsi.org/blogs/auvsi-news/2016/01/29/tornado

[5] BBC Technology. (2016) Google plans drone delivery service for 2017. [Online]. Available: http://www.bbc.com/news/technology-34704868

[6] Jointed Planning and Development Office (JPDO), "Unmanned aircraft systems (UAS) comprehensive plan – a report on the nation's UAS path forward," Federal Aviation Administration, Tech. Rep., 2013.

[7] National Aeronautics and Space Administration. (2016) Challenge is on to design sky for all. [Online]. Available: http://www.nasa.gov/feature/challenge-is-on-to-design-sky-for-all

[8] P. Kopardekar, J. Rios, T. Prevot, M. Johnson, J. Jung, and J. E. R. III, "Uas traffic management (utm) concept of operations to safely enable low altitude flight operations," in *AIAA Aviation Technology, Integration, and Operations Conference*, 2016.

[9] P. Fiorini and Z. Shillert, "Motion planning in dynamic environments using velocity obstacles," *International Journal of Robotics Research*, vol. 17, pp. 760–772, 1998.

[10] G. C. Chasparis and J. S. Shamma, "Linear-programming-based multi-vehicle path planning with adversaries," in *Proceedings of American Control Conference*, June 2005.

[11] J. van den Berg, M. C. Lin, and D. Manocha, "Reciprocal velocity obstacles for real-time multi-agent navigation," in *IEEE International Conference on Robotics and Automation*, May 2008, pp. 1928–1935.

[12] R. Olfati-Saber and R. M. Murray, "Distributed cooperative control of multiple vehicle formations using structural potential functions," in *IFAC World Congress*, 2002.

[13] Y.-L. Chuang, Y. Huang, M. R. D'Orsogna, and A. L. Bertozzi, "Multi-vehicle flocking: Scalability of cooperative control algorithms using pairwise potentials," in *IEEE International Conference onRobotics and Automation*, April 2007, pp. 2292–2299.

[14] E. N. Barron, "Differential Games with Maximum Cost," *Nonlinear analysis: Theory, methods & applications*, pp. 971–989, 1990.

[15] I. Mitchell, A. Bayen, and C. Tomlin, "A time-dependent Hamilton-Jacobi formulation of reachable sets for continuous dynamic games," *IEEE Transactions on Automatic Control*, vol. 50, no. 7, pp. 947–957, July 2005.

[16] O. Bokanowski, N. Forcadel, and H. Zidani, "Reachability and minimal times for state constrained nonlinear problems without any controllability assumption," *SIAM Journal on Control and Optimization*, pp. 1–24, 2010.

[17] O. Bokanowski and H. Zidani, "Minimal time problems with moving targets and obstacles," {*IFAC*} *Proceedings Volumes*, vol. 44, no. 1, pp. 2589 – 2593, 2011.

[18] K. Margellos and J. Lygeros, "Hamilton-Jacobi Formulation for Reach-Avoid Differential Games," *IEEE Transactions on Automatic Control*, vol. 56, no. 8, Aug 2011.

[19] J. F. Fisac, M. Chen, C. J. Tomlin, and S. S. Shankar, "Reach-avoid problems with time-varying dynamics, targets and constraints," in *18th International Conference on Hybrid Systems: Computation and Controls*, 2015.

[20] J. Ding, J. Sprinkle, S. S. Sastry, and C. J. Tomlin, "Reachability calculations for automated aerial refueling," in *IEEE Conference on Decision and Control*, Cancun, Mexico, 2008.

[21] H. Huang, J. Ding, W. Zhang, and C. Tomlin, "A differential game approach to planning in adversarial scenarios: A case study on capture-the-flag," in *Robotics and Automation (ICRA), 2011 IEEE International Conference on*, 2011, pp. 1451–1456.

[22] A. M. Bayen, I. M. Mitchell, M. Oishi, and C. J. Tomlin, "Aircraft autolander safety analysis through optimal control-based reach set computation," *Journal of Guidance, Control, and Dynamics*, vol. 30, no. 1, 2007.

[23] M. Chen, J. Fisac, C. J. Tomlin, and S. Sastry, "Safe sequential path planning of multi-vehicle systems via double-obstacle hamilton-jacobi-isaacs variational inequality," in *European Control Conference*, 2015.
[24] E. A. Coddington and N. Levinson, *Theory of ordinary differential equations*. Tata McGraw-Hill Education, 1955.